SCHWEIZ. MINERAL. PETROGR. MITT. 79, 263–276, 1999

The newly defined "Greenstone Unit" of the Aiguilles Rouges massif (western Alps): remnant of an Early Palaeozoic oceanic island-arc?

by *Christoph Dobmeier*[1], *Hans Rudolf Pfeifer*[2] and *Jürgen F. von Raumer*[3]

Abstract

In the southwestern part of the Aiguilles Rouges massif (pre-Alpine basement of the Helvetic realm, western Alps), a metavolcanic sequence, newly defined as the "Greenstone Unit", is exposed in two N–S trending belts of several 100 metres in thickness. It consists of epidote amphibolites, partly epidote and/or calcic amphibole-bearing greenschists, and small amounts of alkali feldspar-bearing greenschists, which underwent low- to medium-grade metamorphism during Visean oblique collision. Metamorphic calcic amphiboles and epidotes show strong chemical zoning, whereas metamorphic plagioclase is exclusively albitic in composition (An 1–3). The SiO_2 content of the subalkaline tholeiitic to calc-alkaline suite ranges continuously from 44 wt% to 73 wt%, but andesitic rocks predominate. The majority of samples have chemical compositions close to recent subduction-related lavas; some are even restricted to recent oceanic arcs (extremely low Ta and Nb contents, high La/Nb and Th/Ta ratios). But several basaltic to basalto-andesitic samples resemble continental tholeiites (low Th/Ta, La/Nb ratio). As it is very probable that both lava types are to some extent contemporaneous, it is proposed that the Greenstone Unit represents a former oceanic volcanic arc which temporarily underwent extension during which emplacement of continental tholeiite-like rocks occurred. The cause of the extension remains ambiguous. Considering palaeotectonic significance and age of other metavolcanic units in the Aiguilles Rouges massif, the Greenstone Unit most likely formed in the Early Palaeozoic.

Keywords: greenschists, amphibolites, geochemistry, petrography, mineral chemistry, Variscan, western Alps basement, Aiguilles Rouges massif.

Introduction

In 1927, CORBIN and OULIANOFF reported the presence of supposedly "Hercynian" (pre-Carboniferous) amphibolites and greenschists from the Prarion area of the southwestern Aiguilles Rouges External massif (Fig. 1). Later, LAURENT (1967) inferred from a detailed petrographic study, which included some chemical bulk rock analyses, a volcanic origin and maximum metamorphic conditions of 3–4 kb and 600 °C for the rocks, which form the lower and middle unit of the "série de Prarion-Pormenaz" in his lithologic subdivision of the southwestern Aiguilles Rouges massif; the upper unit consists of low-grade metasedimentary rocks. BUJAN (1989) discovered dolomite marbles of several centimetres in thickness in the greenstones near the Prarion summit (Fig. 1b). Based on palaeontologic age data of BELLIÈRE and STREEL (1980) and his own field observations, Bujan separated most probably Upper Visean phyllites and chlorite-sericite schists ("metagraywackes") from the greenstones on the one side, and from Upper Carboniferous detrital rocks on the other side. In his new subdivision, he distinguished between an old basement ("socle ancien", formed by gneisses), a unit comprising *all* occurring greenstones ("roches vertes"), a series of low-grade metasedimentary rocks ("série grise viséenne"), and Westphalian to Stephanian rocks.

[1] Institut für Geowissenschaften, Universität Mainz, D-55099 Mainz, Germany. Corresponding author. <dobmeier@mail.uni-mainz.de>
[2] Université de Lausanne, Centre d'Analyse Minérale, BFSH 2, CH-1015 Lausanne, Switzerland.
[3] Institut de Minéralogie et de Pétrographie, Université de Fribourg, Pérolles, CH-1700 Fribourg, Switzerland.

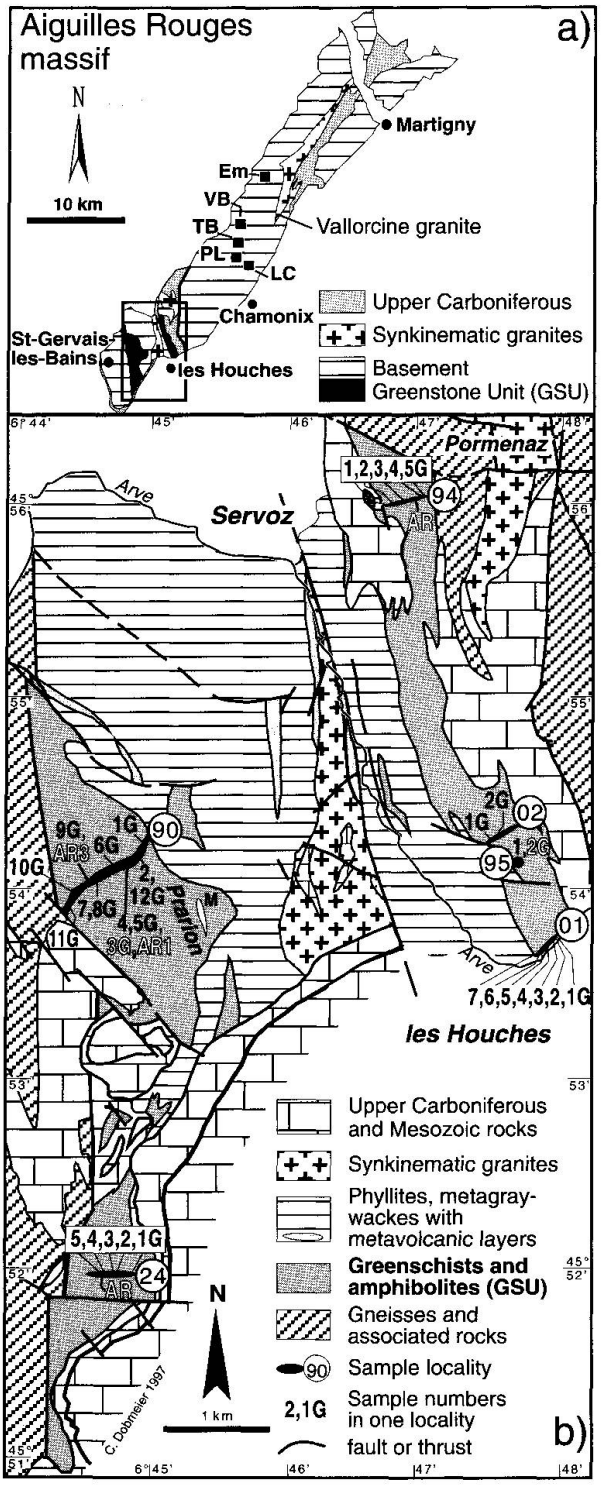

Fig. 1 (a) Geological outline of the Aiguilles Rouges massif. Em – Lac d'Emosson, LC – Lac Cornu, PL – Petit Lac, TB – Tête du Béchat, VB – Val Bérard; box indicates figure 1 b. (b) Lithological subdivision of the southwestern Aiguilles Rouges massif. M – lens of dolomite marble. Numbers indicate sample localities (selected analyses in Tabs 1 and 2). Geographic coordinates (referred to the meridian of Paris, Lambert zone II) of the samples for electron microprobe studies (white numbers): 24-AR 941.985 / 105.545, 90-3G and 90-AR1 941.990 / 109.650, 90-AR3 941.670 / 109.430, 94-AR 944.200 / 113.300, 95-2G 945.840 / 109.070.

According to comparative structural studies, he proposed a Devonian to Early Carboniferous formation of the greenstones.

New structural, petrological and geochemical data enabled DOBMEIER (1996) to present a new subdivision for the southwestern part of the Aiguilles Rouges. Therein, the metavolcanic suite of unknown age constitute the "Greenstone Unit". Its extent largely tallies with Bujan's "roches vertes" but geochemical arguments favour the integration of several small greenstone lenses enclosed by phyllites and metagraywackes within a separate tectonic unit (Fig. 1b).

The aim of this paper is to present new data and interpretations of the newly defined lithotectonic Greenstone Unit with special emphasis on the bulk rock chemistry and its possible geotectonic implications.

Geological setting

The polymetamorphic basement of the Aiguilles Rouges massif (Fig. 1a) is composed of multiplely deformed rocks with highly different maximum P-T conditions. The tectono-metamorphic event is dated by $^{39}Ar/^{40}Ar$ cooling ages (step heating, white micas) which range from 337 ± 3.2 Ma (gneisses, St-Gervais-les-Baines vicinity) to 316 ± 2 Ma (pegmatitic neck filling of amphibolite, Tête du Béchat, DOBMEIER, 1998) and a concordant U/Pb zircon age for the Pormenaz monzogranite which intruded synkinematically at 333 ± 2 Ma while lower greenschist facies conditions persisted (BUSSY et al., 1998; DOBMEIER, 1996; 1998). The Vallorcine granite intruded a still active post-metamorphic shear zone at 307 ± 1.5 Ma (VON RAUMER et al., 1993; concordant U/Pb zircon age, BUSSY and HERNANDEZ, 1997). Upper Carboniferous sediments (Westphalian D to Stephanian ?) which cover unconformably the basement do not bear imprints of a Variscan metamorphism (VON RAUMER et al., 1993; DOBMEIER, 1996).

Metavolcanic rocks are known from several areas of the Aiguilles Rouges massif (Fig. 1a):

(1) Some ultrabasite and eclogite lenses are intercalated in possibly orthogene migmatites around Lac Cornu (PAQUETTE et al., 1989; PFEIFER and VON RAUMER, 1996).

(2) Eclogitic amphibolites and amphibolites appear as lens-shaped bodies of 5 to several 100 metres in length in metasedimentary rocks between Lac d'Emosson and Petit Lac vicinities (VON RAUMER et al., 1990; SCHULZ and VON RAUMER, 1993). At Tête du Béchat, metabasites reach an exceptional thickness of several 100 metres due to multiple folding (own data). In the Val

Bérard, hybrid-type (with I-type affinity) and S-type granitoids intruded this volcanosedimentary assemblage (WIRSING, 1997).

(3) A heterogeneous sequence of epidote amphibolites and partly epidote and/or calcic amphibole-bearing chlorite-albite to albite-chlorite schists forms two N–S trending belts of 300 to over 1000 metres in thickness in the tectonically complicated and lithological diverse southwestern end of the Aiguilles Rouges massif (Fig. 1b). This occurrence, designated as Greenstone Unit (DOBMEIER, 1996; 1998), shall be described in detail.

Lithology – Petrography

The two separate outcrop areas of the Greenstone Unit (Fig. 1b) exhibit considerable differences in their lithological composition. East of the river Arve, mainly chlorite-albite to albite-chlorite schists are exposed. Small epidote amphibolite lenses of a few metres in thickness, intercalations of alkalifeldspar-bearing schists, and amphibole and/or epidote-bearing layers are scarce. On the contrary, west of the Arve, epidote amphibolites and amphibole/epidote-bearing schists are very frequent (see cross-section in Fig. 5).

Dark green, fine grained and homogeneous epidote amphibolites consist of amphibole, epidote, albite, chlorite, sphene, rutile, ore minerals ± quartz. Approaching shear zones, the homogeneous texture changes progressively to a layered texture (e.g. locality 90, Fig. 5), and the SiO_2 content increases from 48–54 wt% to 60 wt%. A 30 metres thick and several hundred metres long epidote amphibolite (samples 90-3G, –1AR; Figs 1b, 5; NW of the Prarion summit) with exceptionally large amphibole crystals (2–3 cm long, 15–25 vol.%) will be referred to as "porphyritic amphibolite".

Greenschists occur in different textural types which can alternate at almost any scale. By far most abundant are two types of chlorite-albite to albite-chlorite schists (Chl + Ab + ore minerals ± Qtz ± Ep ± Amp ± Cal ± Rt ± Sph ± sericite): (1) layered schists (middle to dark green/blue green and white) with millimetric to centimetric layering caused by transposition, and (2) porphyritic schists with a fine grained greenish matrix and white albite porphyroclasts (up to 2 cm in diameter). LAURENT (1967) designated these rocks as "gneiss prasinitiques" and "gneiss ovarditiques", respectively. Although he stated that ovardites should be free of amphiboles and epidotes, we noticed that porphyritic greenschists contain both minerals more frequently than layered greenschists. A very fine grained and occasionally platy type is commonly exposed close to tectonic contacts (e.g. railway station of les Houches, locality 01 in Fig. 1b). Some greenschists contain considerable amounts of sericite (3–10 vol.%) which are often associated with alkalifeldspars (max. 5 vol.%), although highest sericite contents appear in the very fine grained schists close to tectonic contacts; this is most probably a result of feldspar destabilisation due to high shear stress. Quartz-rich layers are characterized by thin quartz veins which mark the foliation. The SiO_2 content of the greeschists varies between 54 and 66 wt%; the majority of the samples are andesites. Sericite-rich (and alkalifeldpar-bearing) samples have SiO_2 contents as high as 72wt%. Garnet appears exclusively in a dacitic amphibole schist in the Prarion area (90-6G). A rhyolitic rock (Qtz–Chl–Ab schist; sample 90-12G) occurs as a few metres thick light green layer in porphyritic and layered greenschists (Figs 1b, 5).

Brownish dolomite layers of about 30 centimetres in thickness are intercalated in greenstones near the Prarion summit (Fig. 1b). A sedimentary origin of the marbles seems likely as the layers contain quartz grains (BUJAN, 1989). In consequence, the greenstones are considered to represent a mainly volcanic sequence (as already concluded by LAURENT, 1967). Several arguments support this assumption:

(1) The average size of matrix grains ranges between 0.1 and 0.3 millimetres. COLOMBI (1989) demonstrated that the average grain size discrimination between basalts and gabbros remains unchanged during metamorphism. For the "porphyritic amphibolite", a subvolcanic or plutonic formation is unlikely because of the matrix grain size (below 0.2 mm).

(2) Mineral contents and textures show considerable and rapid lateral variations typical for volcanic successions.

(3) Some thin sections contain microlithons with textures resembling a primary trachytic texture.

Metamorphism, structural overprint and contacts with neighbouring units

The observed mineral assemblages reflect variable maximum metamorphic conditions. Again, the exposures east and west of the Arve river differ from each other. Rocks exposed east of the river underwent a greenschist facies metamorphism; most metamorphic amphiboles are actinolites or actinolitic hornblendes, and epidote reaches maximum Al^{3+} values of 2.40 per formula unit (p.f.u.). West of the Arve river, Mg-hornblendes and

tschermakitic hornblendes are common, epidote contains up to 2.60 Al^{3+} p.f.u., and garnet is present; altogether, an amphibolite facies metamorphism is indicated. Many minerals of the described peak parageneses suffered retrograde transformations like epidotisation or chloritisation (amphibole, garnet) and a considerable loss of Ti (amphibole, chlorite, rare biotite). Microstructurally controlled geothermobarometry in the system SAFMCN (TRIBOULET, 1992) yields prograde-retrograde clockwise P-T-deformation paths with maximum P-T conditions of 3.25 kb at 440 °C east, and 6.75 kb at 630 °C west of the Arve (DOBMEIER, 1998).

A strong progressive deformation accompanied metamorphism (DOBMEIER, 1998). Main structural features include the subvertical N–S to NW–SE trending pervasive foliation S_2 and the mainly subhorizontal stretching lineation L_2. B_2 buckle fold axes are parallel to L_2. Shear sense indicators prove an uniformly dextral sense of shear parallel to L_2. All in all, a transpressive regime is indicated. Several profiles through the entire rock mass indicate that the unit was neither isoclinally folded at a large scale nor multiplied by internal thrusting (e.g. Fig. 5).

All exposed contacts with neighbouring high-grade gneisses and low-grade phyllites or metagraywackes are subvertical faults and/or mylonitic shear zones.

Mineral chemistry

The composition of the main mineral phases was checked in 6 samples (positions see Fig. 1b) with a CAMECA SX-50 electron microprobe (15 kV accelerating voltage, 15 nA probe current, 20.000 ×

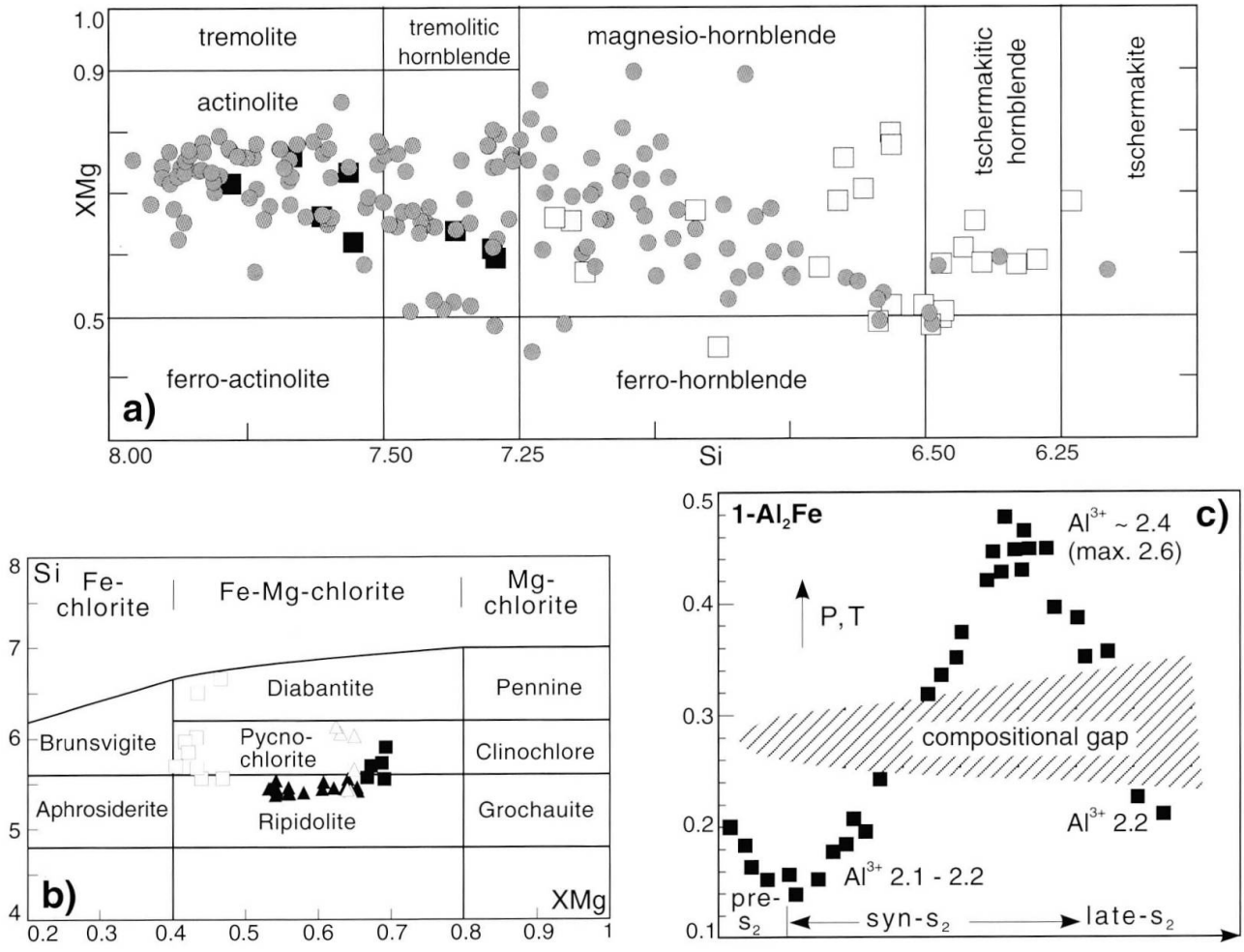

Fig. 2 Chemical composition variations of selected minerals. (a) Amphiboles in the diagram Si vs X_{Mg} for calcic amphiboles after LEAKE (1978). Squares – Ti-rich cores of amphibole 1 in sample 90-AR1, black squares – clear rims of amphibole 1, grey squares – amphibole 1 in sample 95-2G, circles – metamorphic amphiboles (see text). (b) Chlorite analyses in the X_{Mg} vs Si diagram of TRÖGER (1967). Filled triangles – 90-AR1, triangles – 90-AR3, squares – 94-AR, filled squares – 95-2G. (c) Chemical evolution of epidote (1-Al_2Fe) during deformation (Δt) in sample 90-AR1; Al^{3+} given per formula unit (p.f.u.).

enlargement, 30 s counting time, natural standards) at the Institut de Minéralogie, Lausanne. Amphibole structural formulae have been computed with the program NAMPH (provided by C. TRIBOULET, Paris) using the routine of PAPIKE et al. (1974) for the determination of ferric iron. Al^{VI} and Fe^{3+} in epidote have been calculated following LAIRD and ALBEE (1981), additionally including Cr^{3+}. For structural formulae computations of chlorite, all Fe has been considered as Fe^{2+} due to uncertainties caused by possibly existing vacancies and varying Fe^{2+}/Fe^{3+} ratio in different samples. Microprobe analyses are published in DOBMEIER (1996, 1998).

Amphibole: All analyses (Fig. 2a) are calcic amphiboles (LEAKE, 1978). The crystals were separated into several generations (Amp 1–Amp 4) in every sample according to their microstructural positions (separable core or pre-textural / syn-S_1 or pre-S_2 / syn-S_2 / post-S_2).

First generation "amphiboles" (Amp 1) of the porphyritic amphibolite (90-3G, 90-1AR) are composite grains composed of Ti-rich Mg-hornblende (max. 3.6 wt% TiO_2), albite and sphene (10 vol.%). The acicular sphenes which cause the brownish colour of the grains are oriented preferentially in the cleavages of Mg-hornblende. This argues for the formation of Amp 1 through a retrograde reaction

Amp 0 → (Mg-hornblende + Ab + Sph) = Amp 1.

Re-calculated Amp 0 have TiO_2 contents as high as 7.5 wt%. Such high values are known only in kaersutite, a magmatic amphibole (DEER et al., 1963). Therefore it is concluded, that Amp 1 represent altered magmatic amphiboles. In the interior of some grains partly rectangular areas exist of a few microns in length, which show uncommon compositions and a zonation: The rims are always formed by actinolite whereas the cores consist of albite and clinozoisite or albite and chlorite. The original mineral phase remains unknown.

All metamorphic amphiboles (Amp 2–Amp 4), varying from actinolite to Mg-hornblende or tschermakite, are chemically zoned. Prograde and retrograde trends are present. Only late/post-kinematically grown acicular Amp 4 is unzoned actinolite. Several crystals have been studied with three profiles set in 60° distance to check whether the zonations are primary grown or caused by secondary alteration (lamellae); the rim parallelity of all zonations suggests their primary origin.

Feldspars of the albite-plagioclase family vary between An_0 and An_{42}. The An-contents of the crystals exhibit spatial and microstructural variations. In samples collected east of the Arve river only albite ($An_{0.2-2.7}$) is present, whereas more westward situated samples additionally bear crystals richer in An-component (up to An_{42}). But all grains clearly grown during metamorphism are albitic (max. An_8) and all grains in a pre-foliation microstructural position are oligoclase or andesine.

Alkali feldspars (Or_{77-96}) have been identified by EMS only in sample 95-2G. Generally, the crystals show no chemical zonation. Surprisingly, innermost albite porphyroclast cores of porphyritic chlorite-albite schists are sporadically very potassium-rich. The change from orthoclase to albite is always sharp.

Epidote: As the content of the pure Fe^{3+} component $FeAl_2$ varies between 38 and 86 mol%, all crystals are epidote s.s. (DEER et al., 1986). All grains show zonations with the substitution $Al_2O_3 \rightleftarrows FeO^*$ as the only significant variation. Al^{3+} increases or decreases (Fig. 2b) from core to rim depending on the microstructural position of the analyzed crystal, thus reflecting changing P-T conditions during growth (RAITH, 1976).

Chlorite is omnipresent. X-ray diffractometry on powder samples showed that the IIB-polytype dominates in all samples. According to the nomenclature of TRÖGER (1967), the analyzed crystals belong to the Fe–Mg chlorites (mainly pycnochlorite or ripidolite, Fig. 2c).

Sphenes occupy all microstructural positions and show a high variety in grain shape ranging from rounded grains (early growth) to large rhombic crystals which partly post-date the main foliation. Occasionally, optically identified sphene appears as rim around an opaque core. Surprisingly, cores and rims however have almost identical chemical compositions, although the rims have slightly lower TiO_2 contents (36.3–38.6 wt%) than the opaque cores (39.1–39.6 wt%).

Whole rock chemistry

A total of 75 samples were collected and 39 of them were analyzed by X-ray fluorescence and complementary methodes for 34 major and trace elements at the Centre d'Analyse Minérale, University of Lausanne using a Philips PW 1400 spectrometer (for representative analyses see Tabs 1 and 2). Trace elements were analyzed on pressed powder pellets and major elements on glass discs. The water content was calculated from the loss on ignition data, photometric FeO, and coulometric CO_2 analyses. 44 trace elements have been independently determined by ICP-MS for 17 selected samples by K. Govindaraju at the CRPG Laboratoire de Spectrochimie et de Géostandards, Vandœuvres-lès-Nancy, France.

Tab. 1 Representative bulk rock compositions of the metavolcanics of the Greenstone Unit. B – basalt, BA – basaltic andesite, ATH – tholeiitic andesite, ACA – calc-alkaline andesite, D – dacite, RD – rhyodacite, R – rhyolite, d.l. – detection limit (unknown values), n.a. – not analyzed. Trace element contents showing decimals have been analyzed by ICP-MS. Sample 94-1G has been analyzed by XRF only.

Sample	90-AR1	90-3G	90-8G	94-4G	94-AR	90-AR3	90-9G	90-2G	90-1G	95-2G	94-5G	150-1G	90-6G	94-1G	90-12G
Rock type*	B	B	B	BA	BA	BA	BA	ATH	ATH	ACA	ACA	D	D	RD	R
Major oxides (wt%) [XRF]															
SiO_2	44.20	46.04	46.44	51.91	51.95	52.47	53.00	53.88	53.93	58.06	59.63	62.26	62.64	66.69	72.86
TiO_2	1.02	1.52	1.05	1.58	1.99	0.54	0.77	1.30	1.70	0.56	0.39	0.78	0.89	0.68	0.34
Al_2O_3	17.59	17.17	14.79	16.12	15.34	16.19	16.55	15.93	16.01	16.69	16.32	17.85	14.81	15.61	14.12
Fe_2O_3	3.40	3.43	3.22	2.76	5.09	2.54	2.29	2.67	2.62	2.51	2.35	2.17	2.37	0.95	1.02
FeO	6.72	7.72	7.16	6.61	4.87	4.98	4.98	6.76	6.72	3.23	3.54	3.53	6.96	2.87	1.58
MnO	0.15	0.20	0.20	0.16	0.13	0.10	0.17	0.15	0.16	0.09	0.10	0.08	0.29	0.08	0.04
MgO	9.87	8.91	7.08	5.86	3.71	6.99	6.96	5.82	4.42	4.85	4.39	2.32	2.90	2.23	1.26
CaO	8.14	8.00	10.83	5.19	5.63	5.36	7.02	3.52	4.80	6.38	5.45	0.19	2.64	0.72	0.27
Na_2O	2.53	2.20	2.66	4.85	6.28	5.42	4.59	4.87	3.19	4.84	4.37	2.57	4.17	5.72	6.74
K_2O	0.83	0.54	0.56	0.50	0.65	0.71	0.53	0.04	0.95	0.22	0.75	4.03	0.23	0.94	0.49
P_2O_5	0.11	0.19	0.20	0.20	0.24	0.05	0.05	0.11	0.31	0.08	0.03	0.11	0.15	0.14	0.05
H_2O	4.28	3.72	2.44	2.78	3.17	2.56	1.81	3.14	3.08	2.04	1.92	3.24	2.28	1.94	1.30
CO_2	0.36	0.21	3.51	0.82	0.52	0.57	0.76	1.44	1.30	0.09	0.74	0.14	0.10	0.74	0.13
Total	99.19	99.85	100.14	99.34	99.56	98.44	99.48	99.63	99.19	99.64	99.98	99.26	100.43	99.31	100.20
Mg-number	0.59	0.54	0.50	0.47	0.43	0.58	0.58	0.46	0.40	0.60	0.55	0.40	0.29	0.44	0.44
Trace elements (ppm) [XRF/ICP-MS]														[XRF]	
Hf [ICP-MS]	1.93	2.25	1.72	3.25	4.26	1.24	1.30	2.50	4.88	1.74	1.49	5.21	4.69	< d.l,	4.79
Zr	53	67	59	132	155	32	35	84	191	44	33	179	163	122	143
Ta [ICP-MS]	0.27	0.36	0.05	0.30	0.40	0.04	0.04	0.09	1.04	0.06	0.03	0.95	0.12	n.a.	0.15
Nb [ICP-MS]	3.39	4.76	0.48	3.66	5.02	0.39	0.45	1.17	13.20	0.71	0.29	11.00	1.36	< d.l.	1.43
Y	11	17	25	26	35	8	20	23	37	15	7	24	47	7	20
CS [ICP-1MS	2.34	1.54	0.78	4.96	3.18	4.38	1.44	0.82	4.30	0.75	2.45	8.04	0.85	n.a.	1.01
Rb	18	13	11	19	9	22	12	0	24	9	31	129	7	52	9
Sr	380	408	90	146	227	157	193	77	216	364	318	45	54	74	59
Ba	87	151	90	231	310	62	127	29	374	274	127	762	35	399	9.26
Be	< d.l.	0.45	0.06	1.19	0.40	0.54	0.12	0.83	1.09	0.84	0.51	1.93	< d.l.	n.a.	1.07
Cr	49	142	239	65	20	226	275	44	109	110	80	63	54	47	7
Ni	56	38	71	15	14	44	94	11	46	54	83	30	31	39	11
U	0.25	0.24	1.47	0.25	0.39	0.21	0.33	0.28	1.26	0.49	0.35	2.90	0.27	< d.l.	1.20
Th	0.56	0.40	0.10	0.46	0.62	0.24	0.11	0.30	3.07	0.40	0.32	9.11	0.31	< d.l.	1.56
Pb	2.83	2.95	2.03	2.44	33.30	1.87	1.39	20.20	9.40	3.21	6.32	4.18	3.66	< d.l.	1.12
Ga	15	15	12	16	18	14	14	19	18	16	12	21	18	16	11
Zn	98.00	125.00	80.60	96.60	90.80	58.90	57.70	150.00	106.00	42.00	51.10	81.10	254.00	37	40.70
Cd	0.17	0.32	0.37	0.08	0.13	0.11	0.17	0.08	0.22	0.12	0.06	0.09	0.28	n.a,	0.03
Cu	25.00	4.11	2.58	22.80	335.00	2.42	115.00	12.80	52.50	41.40	91.30	33.20	44.90	< d.l.	4.45
CO	67	62	50	38	37	41	39	43	41	25	26	20	27	13	7
V	103	166	248	266	268	194	207	238	190	151	128	134	114	120	45
S	< 10	51	67	129	1527	< 10	100	61	332	75	71	< 10	393	95	88
W	1.43	4.09	3.46	2.00	4.62	3.54	2.40	2.83	5.02	8.54	35.40	3.59	11.90	n.a.	9.76
Mo	0.12	0.43	0.05	0.29	0.39	0.03	0.19	0.25	1.04	0.22	0.86	0.25	0.83	n.a.	0.16
Sn	0.83	1.10	0.56	1.13	1.93	0.46	0.67	0.93	2.47	0.60	0.39	2.61	1.21	n.a.	2.43
Ge	1.03	1.25	0.82	1.44	1.45	1.41	1.17	1.12	1.66	1.39	0.94	1.67	1.04	n.a.	0.96
1n	0.03	0.06	0.06	0.07	0.09	0.03	0.05	0.06	0.08	0.03	0.02	0.06	0.08	n.a.	0.02
As	1.15	0.62	0.84	6.66	17.00	1.94	3.74	2.05	2.01	3.48	1.48	1.18	0.72	n.a.	2.06
Sb	0.44	0.52	0.20	3.15	7.02	1.38	0.63	0.30	1.61	1.55	3.15	2.07	0.31	n.a.	0.78
Bi	0.01	0.03	<d.l.	0.04	0.17	0.01	0.03	0-08	0.13	0.03	0.02	0.13	0.07	n.a.	0.04

* according to anhydrous recalculated SiO_2 content

Chemical changes of the whole rock composition

Investigations on protoliths and primary tectonic environments of metamorphic magmatites are hampered by selective element mobilities caused by rock-fluid interaction during metamorphism/metasomatism. Especially large-ion-lithophile elements (LILE) are affected (THOMPSON, 1991), whereas high-field-strengh elements (HFSE) and the rare earth elements (REE) are considered to remain relatively stable (FLOYD et al., 1996; GAUCH, 1989). For the Greenstone Unit,

Tab. 2 REE analyses of selected samples from the Greenstone Unit. B – basalt, BA – basaltic andesite, A – andesite, D – dacite, R – rhyolite.

Sample	90-AR1	90-3G	90-8G	94-4G	94-AR	90-AR3	90-9G	90-2G	90-1G	95-2G	94-5G	150-1G	90-6G	90-12G
Rock type*	B	B	B	BA	BA	BA	BA	ATH	ATH	ACA	ACA	D	D	R
Rare earth elements (ppm) [ICP-MS]														
La	4.99	6.62	1.69	6.48	10.13	1.71	2.47	2.07	21.17	4.93	2.35	33.96	5.14	6.41
Ce	12.71	17.03	5.74	19.06	27.67	5.32	6.70	6.65	49.65	11.93	5.84	72.03	16.18	17.08
Pr	1.77	2.47	1.03	2.85	4.29	0.85	1.11	1.10	6.36	1.70	0.84	8.68	2.65	2.32
Nd	8.47	11.94	5.96	13.45	21.49	4.15	5.81	6.39	27.88	7.91	3.90	34.89	14.42	10.32
Sm	2.52	3.58	2.43	3.79	6.50	1.34	2.05	2.53	6.86	2.22	1.17	7.33	5.24	2.81
Eu	1.12	1.53	0.85	1.34	2.15	0.49	0.95	0.79	2.05	0.96	0.50	1.65	1.50	0.50
Gd	2.27	3.25	3.01	3.73	6.32	1.38	2.40	2.63	6.20	2.19	1.18	5.63	5.75	2.63
Tb	0.40	0.58	0.59	0.71	1.12	0.27	0.47	0.56	1.08	0.38	0.22	0.84	1.14	0.48
Dy	2.58	3.42	4.15	4.75	6.60	1.79	3.08	3.84	6.57	2.29	1.32	4.71	7.44	3.32
Ho	0.56	0.78	1.01	1.05	1.66	0.46	0.80	0.95	1.46	0.56	0.29	1.00	1.83	0.82
Er	1.36	1.91	2.54	2.66	3.85	1.17	1.90	2.52	3.76	1.32	0.77	2.67	4.68	2.23
Tm	0.19	0.27	0.39	0.40	0.56	0.18	0.29	0.41	0.53	0.17	0.14	0.47	0.75	0.36
Yb	1.30	1.83	2.52	2.69	3.77	1.13	2.00	2.74	3.69	1.21	0.78	2.98	4.93	2.32
Lu	0.18	0.25	0.39	0.43	0.61	0.21	0.35	0.46	0.59	0.22	0.13	0.52	0.77	0.38
Σ_{REE}	40.42	55.46	32.30	63.39	96.72	20.45	30.38	33.64	137.85	37.99	19.43	215.40	72.42	51.98

* according to anhydrous recalculated SiO_2 content

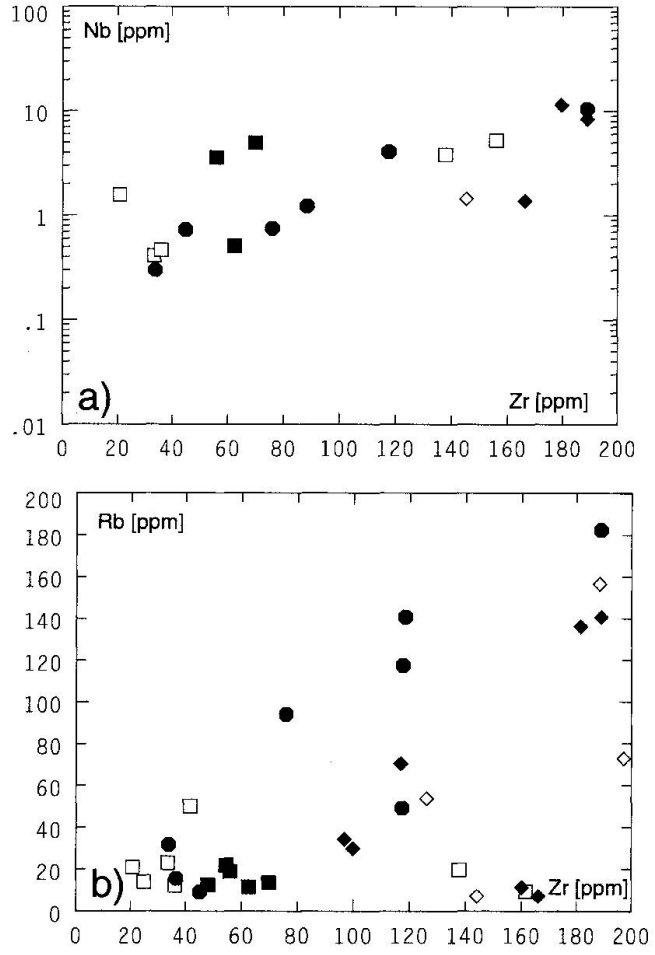

Fig. 3 (a, b): Distribution of stable (Nb) and mobile (Rb) elements relative to Zr in the Greenstone Unit. Filled squares – basalt, squares – basaltic andesite, filled circles – andesite, filled diamonds – dacite, diamonds – rhyodacite and rhyolite (rock names according to anhydrous recalculation).

pairs of incompatible elements (e.g. Fig. 3a) show generally good linear correlations and REE smooth normalized patterns (Fig. 5). Therefore, the elements Zr, Nb, Ta, Y and the REE are regarded as reflecting the primary magmatic composition.

For further studies on element mobilities, all analyzed elements and oxides were plotted against Zr and the Mg-number. Using the argument that good linear correlations indicate little secondary change, Ga, Th, FeO* (FeO + Fe_2O_3), MnO, and P_2O_5 can be considered as unaltered. The two correlation trends in the diagram Zr vs TiO_2 (Fig. 4b) will be discussed below. As some samples do not fit in either trend, selected secondary Ti-alteration may have occurred (FIELD and ELLIOT, 1974; FRISCH et al., 1987). The transition elements (Cr, Ni, Co) vary generally with the Mg-number, although variation is not smooth. All LILE, Na_2O, K_2O and CaO scatter considerably (Fig. 3b) reflecting their general mobility during metamorphism/metasomatism. However, this is not valid for CaO in metabasalts.

Chemical characterization of the magmatic suite

The SiO_2 content varies continuously between 44.20 and 72.86 wt% (Tab. 1, Fig. 4a). Although silica is considered as mobile, ratios between stable incompatible elements (e.g. Nb/Y vs Zr/ TiO_2, WINCHESTER and FLOYD, 1977) confirm the absence of a compositional gap and indicate the subalkaline character of the entire suite. According to their bulk chemical compositions, all basalts and

andesitic basalts and some andesites (e.g. 90-1G, -2G) are unequivocally tholeiitic, whereas other andesites and SiO_2-richer rocks have calc-alkaline compositions. However, the diagrams FeO*/MgO vs FeO* and FeO*/MgO vs TiO_2 (MIYASHIRO, 1974) fail to separate both groups as the FeO*/MgO ratio is generally smaller than 2.5. The diagram Zr vs TiO_2 (Fig. 4b) seems to be a good discriminant between the two compositional trends. Therein, mafic samples define a tholeiitic trend, and dacitic to rhyolitic samples define a calc-alkaline trend which shows no marked enrichment in TiO_2 (and FeO*) with fractionation;

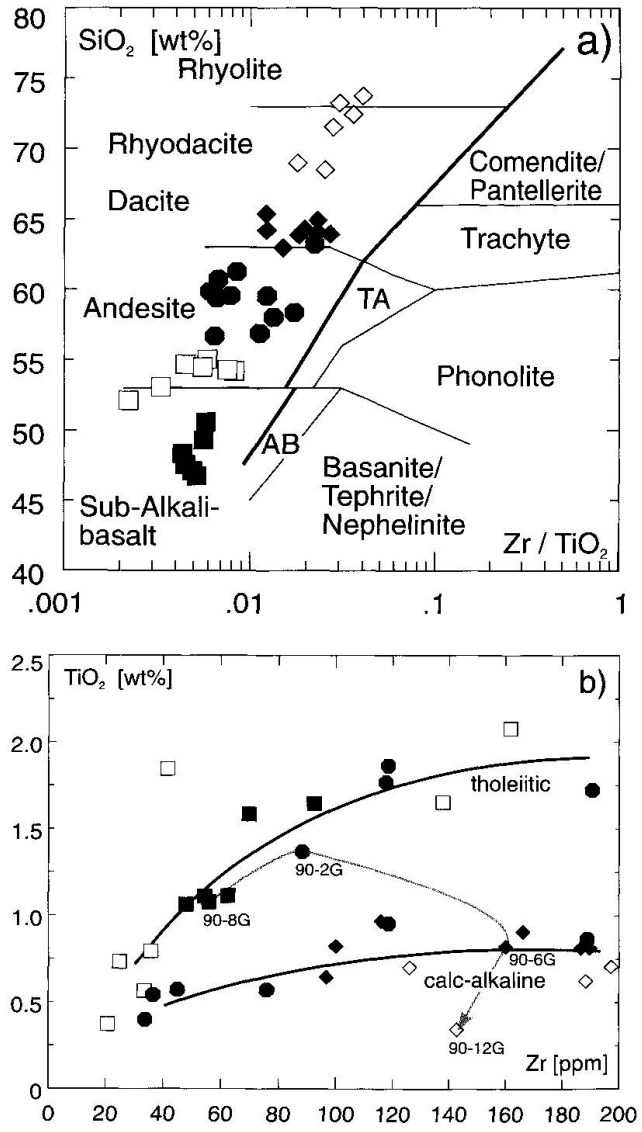

Fig. 4 (a) Zr/ TiO_2 vs SiO_2 diagram (WINCHESTER and FLOYD, 1977) for lava-type designation. All plotted samples are subalkaline. Symbols see figure 3, TA – Trachyandesite, AB – Alkalibasalt. (b) Separation of two chemical trends in the diagram Zr vs TiO_2. Symbols as in figure 3. Numbers indicate samples along an assumed fractional crystallization trend (grey arrow).

andesitic samples are situated along both trends. Calc-alkaline andesites have generally lower abundances of TiO_2, P_2O_5, Nb, and Zr, and lower Ti/V ratios (18–35), but higher Cr and Ni contents and La/Nb ratios (5–8) than tholeiitic andesites (Ti/V 31–56, La/Nb 1.6–2.2). A comparison of C1 chondrite-normalized REE patterns (Fig. 6) depicts considerably lower REE contents and lower La/Sm (1.3–1.5) but equal Gd/Lu ratios (1.1–1.3) in calc-alkaline andesites. However, the diagram is complicated by the samples 90-6G (dacite) and 90-12G (rhyolite) which plot among the calc-alkaline samples but may rather belong to the tholeiitic group: sample 90-6G exhibits C1 chondrite-normalized REE patterns (Fig. 5), and Th/Yb and Ta/Yb ratios (Fig. 8) similar to tholeiitic samples 90-8G and 90-2G. These features strongly indicate consanguinity of the samples. The relative loss of Ti in sample 90-6G may be explained by fractional crystallization of a Ti-retaining mineral phase like amphibole or magnetite/ilmenite (PEARCE and NORRY, 1979). Following the criteria of LEAT et al. (1986), the low-K rhyolitic sample 90-12G is also tholeiitic.

C1 chondrite-normalized REE patterns of *tholeiitic rocks* show either enrichment or depletion for the light REE (La_N/Sm_N 2.85–0.45), whereas the heavy REE vary less (Gd_N/Lu_N 1.56–0.71). The REE content (20.44–177.36 ppm) correlates strictly negatively with the Mg-number (0.67–0.22) in every outcrop except locality 90 (Fig. 1b) where two different REE patterns are present in a roughly complete transection through the Greenstone Unit (Fig. 5).

1. The first pattern is moderately enriched in REE and the normalized concentrations decrease broadly continuously from La to Lu (with $(La/Sm)_N$ 1.2–2.0, $(Gd/Lu)_N$ 1.3–1.6). The andesitic sample 90-1G is shifted towards higher REE concentrations, as can be expected by fractional crystallization. The positive Eu-anomaly (Eu/Eu^* + 2.94) in sample 90-AR1 points to plagioclase cumulation.

2. Low REE abundances, an unfractionated chondritic distribution of the heavy medium REE ($(Gd/Lu)_N$ 0.71–0.95) and depletion in light REE ($(La/Sm)_N$ 0.45–0.63) characterize the second pattern. Again, fractional crystallization may account for increased REE contents in higher differentiated samples.

N-type MORB-normalized multi-element patterns (Fig. 7) for analyses with basaltic composition are generally enriched in LILE (e.g. Cs 709–111x, Sr 4.5–1.0x). The two distinct REE patterns are mirrored by two different HFSE (+REE) distribution patterns. The towards Lu continuously declining REE pattern is associated

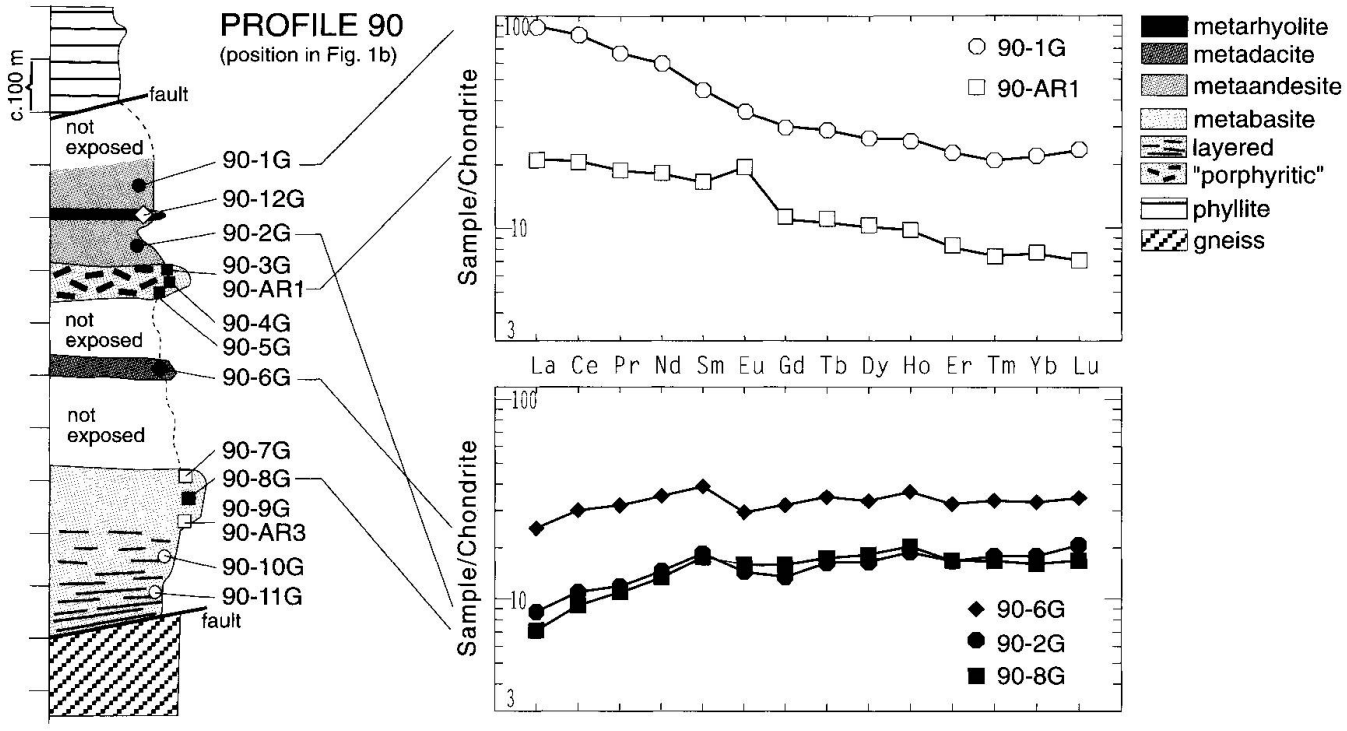

Fig. 5 C1 chondrite-normalized REE patterns (values from SUN and MCDONOUGH, 1989) for profile 90 (position see Fig. 1b). The plotted samples indicate the presence of two chemical trends. White circles – basalt with varied SiO_2 contents located in a high strain zone. Other symbols as in figure 3.

with a marked Th-enrichment and a smooth distribution of other HFSE which have abundances generally above the normalization values (Figs 7a, b). Light-REE-depleted samples exhibit abundances below the normalization values (1.0–0.3x) and a pronounced Nb ± Ta negative anomaly as characteristic features (Fig. 7c).

The diagram Ta/Yb vs Th/Yb of PEARCE (1983) shows also two clearly separated clusters each comprising tholeiitic and calc-alkaline samples (Fig. 8). Obviously, the Greenstone Unit comprises two lava series. The co-existence of tholeiitic and calc-alkaline rocks in each series can be explained by fractionation of a single magma source. It is important to note that both series form voluminous magmatic bodies which are intercalated. This implies their concurrent formation. However, the spatially restricted appearance of samples characterized by the towards Lu continuously declining REE pattern (cf. lithologic column in Fig. 5) suggests that the formation of this lava series occurred not throughout the entire magmatic episode.

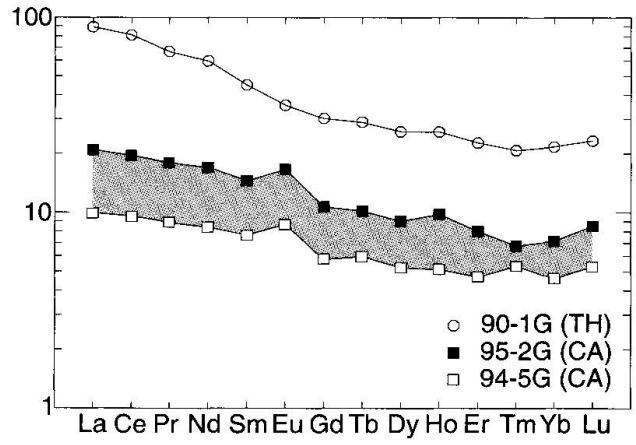

Fig. 6 C1 chondrite-normalized REE patterns (values from SUN and MCDONOUGH, 1989) for andesitic samples.

Lava type discrimination and possible palaeotectonic settings

In the diagramm Ta/Yb vs Th/Yb (Fig. 8) basaltic samples of the lava series with very low Ta + Nb contents and light-REE depletion plot in the field of subduction- related lavas on the "depleted" side of the diagram whereas basalts from the other series fall in the array of within-plate basalts and E-type MORB situated on the "enriched" side of the diagram. Higher differentiated samples of both groups follow a trend of Th-enrichment. The position of a few andesitic basalts in-between the two clusters may be explained by fractional

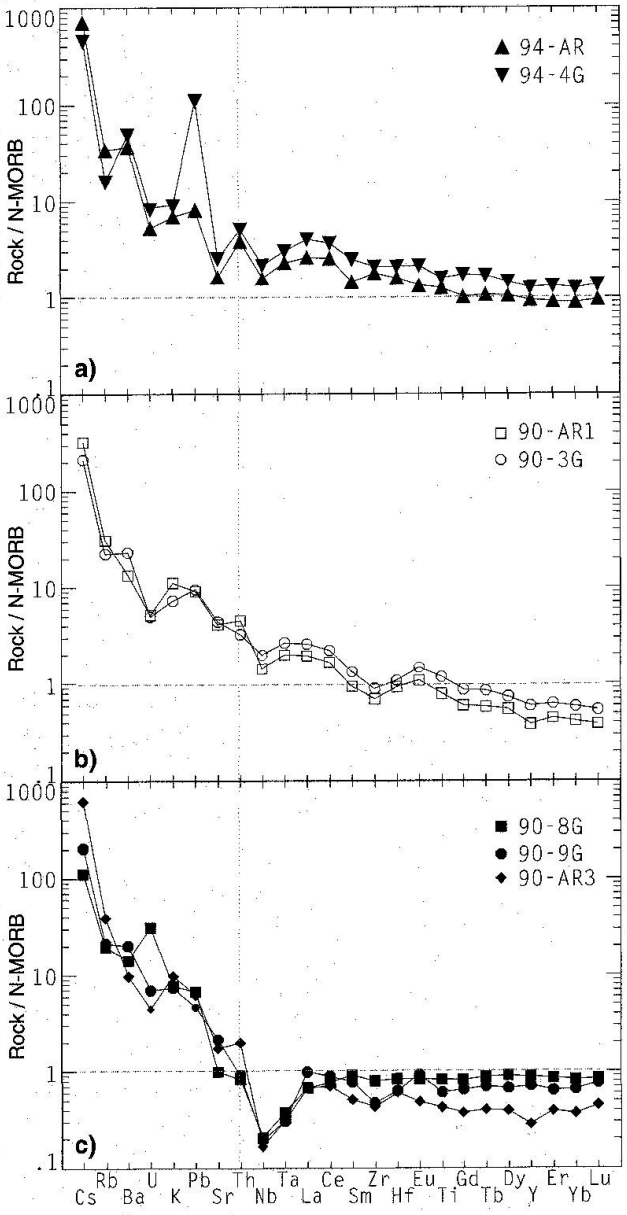

Fig. 7 N-type MORB-normalized multi-element patterns for basaltic analyses (values from SUN and MCDONOUGH, 1989). The elements are arranged in two groups with the potentially mobile elements Cs to Sr on the left side, and immobile elements (Th–Lu) on the right side; the incompatibility of the elements in MORB-source mantle decreases to the right within each group. (a) Samples from the area east of the river Arve. (b) "Enriched" analyses, locality 90 (compare Fig. 6). (c) Primitive ("depleted") tholeiitic analyses from locality 90.

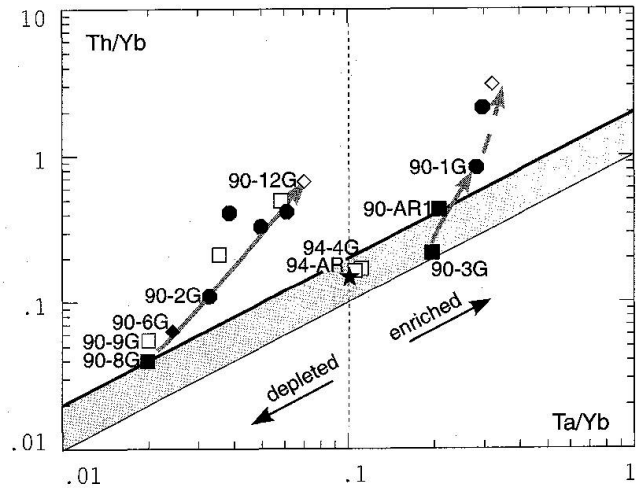

Fig. 8 Ta/Yb vs Th/Yb diagram (PEARCE, 1983). Dashed line separates rocks which are either depleted (left) or enriched (right) in comparison to the primordial mantle composition (star). The shaded field demarcates the array of basalts from non-subduction settings (within-plate basalts and E-type MORB on the enriched side, and N-type MORB on the depleted side). Orogenic (Th-enriched) lavas plot above this field. Thick black line represents chondritic Th/Ta ratio (see HOFMANN, 1988). Grey arrows connect probably comagmatic samples. Symbols as in figure 3.

crystallization within the "enriched" source or by mixing of magmas from both sources (see also Fig. 9a).

The trace element composition of the "depleted" basalts is transitional between N-type MORB and island-arc basalts and may point to a back-arc origin (Fig. 9a). But their extremely low Nb and Ta contents (Fig. 7a) and Ta/Yb ratios at high La/Nb ratios (3–5) are only known from recent oceanic arcs (WOOD et al., 1981; PEARCE, 1983). The typical island-arc compositons (Tab. 1, Fig. 9b) of associated andesites counter also a back-arc basin setting (WILSON, 1989). REE contents of these andesites range within values for "oceanic" andesites from island-arcs (CULLERS and GRAF, 1984) and convex REE pattern for dacitic rocks (as exhibited by sample 90-6G, Fig. 6) are known only from dacites of oceanic island-arcs (CULLERS and GRAF, 1984). Thus, eruption in an oceanic island-arc setting is most likely for this lava series. The extremely low Ta–Nb contents in the basic rocks probably results from a depleted nature of the oceanic mantle as the N-type MORB-normalized multi element patterns (Fig. 7a) show normalized Th contents similar to normalized contents of the other HFSE and REE (GILL, 1981). However, contamination of the mantle by Th-rich fluids derived from a subducted plate cannot be excluded as Th/Yb ratios for basic members vary considerably (PEARCE, 1983).

Basaltic samples of the "enriched" series plot in the field of continental tholeiites in the diagram $(Th/Ta)_N$ vs $(Tb/Ta)_N$ of THIÉBLEMONT et al. (1994) which allows the distinction between E-type MORB and continental tholeiites (Fig. 9a). Higher differentiated rocks of this series are situated at or in the field for felsic lavas associated

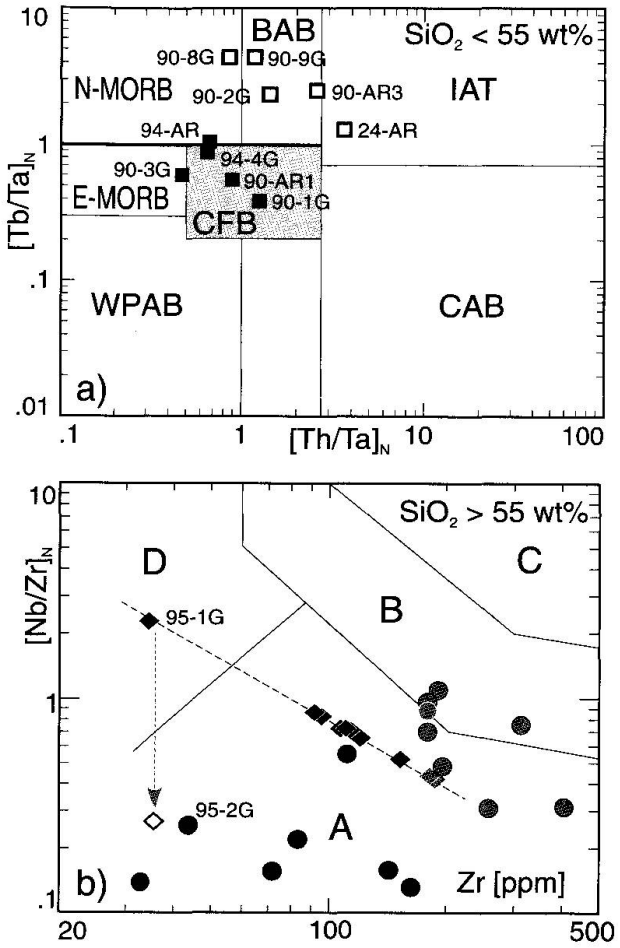

Fig. 9 Lava type discrimination. (a) $(Th/Ta)_N$ vs $(Tb/Ta)_N$ diagram for mafic rocks (THIÉBLEMONT et al., 1994). Normalisation values are 0.0351 ppm for Ta, 0.094 ppm for Tb, and 0.082 ppm for Th (from HOFMANN, 1988). BAB – back-arc basalt, CAB – calc-alkaline basalt, CFB – continental tholeiite, E-MORB – E-type MORB, IAT – island-arc tholeiite, N-MORB – N-type MORB, WPAB – within-plate alkaline basalt. Squares – samples with unfractionated C1 chondrite-normalised REE distribution pattern, filled squares – samples with LREE enrichment (compare Fig. 5). (b) Zr vs $(Nb/Zr)_N$ diagram for differentiated rocks (THIÉBLEMONT and TÉGEY, 1994). Normalisation values are 0.6175 ppm for Nb and 9.714 ppm for Zr (from HOFMANN, 1988). A – volcanic arc and back arc lavas, B – calc-alkaline and alkaline rocks emplaced in continental collision zones, and felsic lavas associated with continental tholeiites, C – within-plate alkaline rocks, D – collision-related peraluminous lavas. Filled circles – samples with known Nb content, filled diamonds – XRF analyses containing Nb below the detection limit of 5 ppm. For these samples 5 ppm Nb content was assumed, resulting in highest expectable Nb/Zr ratios; the dashed line connects these analyses. The chemically very similar samples 95-1G (XRF) and 95-2G (ICP-MS) may illustrate the difference between unknown and known Nb value; a vertical arrow connects the calculated value for sample 95-1G with an expectable value (diamond) for the same sample as deduced from sample 95-2G. Grey filled symbols – samples associated with continental tholeiites.

with continental tholeiites/calc-alkaline to alkaline rocks of continent-continent collision zones in the diagram Zr vs $(Nb/Zr)_N$ (Fig. 9b). As both lava series formed simultaneously, a continent-continent collision setting can be excluded. In consequence, the "enriched" samples represent a continental tholeiite-like lava series. Continental tholeiites indicate an extensional tectonic regime rather than a particular palaeotectonic setting.

It remains to explain the contemporaneous eruption of continental tholeiites and island-arc volcanics. One possibility is the formation of a marginal basin for which the association of arc-type and within-plate lavas is a common feature (HAWKESWORTH et al., 1977; WOOD et al., 1981; WILSON, 1989; TSUCHIYA, 1990). Although the composition of many samples from the island-arc series contradicts this interpretation, it remains viable as the continental tholeiites formed most probably not throughout the arc formation. In consequence, marginal basin formation could have occurred incipiently at the beginning or at the end of the magmatic episode. An alternate explanation is the subduction of a spreading center. LAGABRIELLE et al. (1994) describe a volcanic sequence composed of E-type MORB and Nb-depleted basalts, andesites and dacites from the Taito Peninsula of southern Chile. Although this sequence erupted on continental crust, its chemical composition is strikingly similar with the Greenstone Unit.

Composition and palaeotectonic setting of metavolcanic units from other External massifs

Metavolcanic bodies of comparable size exist only in the southwestern domain of the adjacent Belledonne External massif:

(1) The Cambro-Ordovician Chamrousse-Séchillienne ophiolitic complex is a typical ophiolitic sequence dominated by ultramafics and layered gabbros. Geochemical arguments suggest emplacement at an attenuated passive margin or in a back-arc basin (MÉNOT, 1987; 1988).

(2) In the Rioupéroux-Livet formation, metabasalts, rare felsic metavolcanic rocks and some metapelites are associated with Late Devonian trondhjemitic plutons (MÉNOT, 1987; 1988). Preserved field evidence of uncomplete magma mixing proves magma bimodality. The geochemical significance is under debate: CARME and PIN (1987) argued for an active margin environment, whereas MÉNOT (1987) proposed emplacement within an attenuated crust during continent-continent collision. In comparison with the Greenstone Unit, the metabasalts of the Riou-

péroux-Livet formation are considerably richer in REE and HFSE, and the Ta–Nb negative anomaly is much less pronounced.

(3) Geochemical data for the Allemont-Rochetaillée subunit, composed of metadetrital sediments and amphibolites (CARME and PIN, 1987; MÉNOT, 1987; 1988), are very limited. CARME and PIN (1987) report Th, Nb and Zr anomalies in the metabasalts and assume a magmatic evolution controlled by a subduction zone. Their proposed Late Proterozoic to Early Palaeozoic age (based on preliminary U/Pb zircon data) is yet to be confirmed.

None of these units shares a corresponding lithological composition or an indisputably similar geochemical signature with the Greenstone Unit. Hence, correlation attempts seem sensible only after ascertainment of an absolute age for the latter.

Conclusions and discussion

In the Latest Visean, the Greenstone Unit underwent a Barrovian-type greenschist to amphibolite facies metamorphism which was most probably responsible for secondary minor changes in bulk rock compositions, although a late metasomatism cannot be ruled out. Especially LILE were affected whereas HFSE, REE, and several other trace and major elements remained stable. This enabled investigations on the chemical character and palaeotectonic setting of the metavolcanic rocks. The subalkaline suite comprises mafic to felsic tholeiitic and intermediate to felsic calc-alkaline lavas, and can be divided in a predominantely mafic "enriched" lava series which is correlative with continental tholeiites and a mafic to felsic "depleted" lava series of strong oceanic island-arc affinity (Figs 7, 8). The latter constitutes the major portion of the Greenstone Unit. Both lava types erupted obviously simultaneously as they now form an alternate sequence of voluminous effusive bodies (Fig. 5). Thus the distinct disparity in petrochemical character strongly indicates that the two identified series have independent magma sources and most likely do not reflect either the extent of partial melting or fractionation of a single magma source. As the continental tholeiite-like rocks appear only in the eastern part of outcrop 90 (Fig. 1b, lithologic column in Fig. 5), their eruption may have occurred in a restricted time interval either early or late during arc formation. The episode of tectonic extension indicated by their presence could be associated with either incipient development of a marginal basin (HAWKESWORTH et al., 1977; WOOD et al., 1981; TSUCHIYA, 1990) and/or subduction of a spreading center (HIBBARD and KARIG, 1990; LAGABRIELLE et al., 1994).

So far, no magmatic age has been determined radiometrically. BUJAN (1989) reported a similar deformation and metamorphic overprint for the greenstones and adjacent phyllites. This and a proposed Late Visean age for the phyllites (BELLIÈRE and STREEL, 1980) let him to assume a Devonian to Early Carboniferous eruption age. However, several of our results are inconsistent with such a conclusion. Very contrasting peak metamorphic conditions in the greenstones and the neighbouring phyllites (especially west of the Arve river) and the presence of tectonic contacts suggest that these rocks belong to different lithotectonic units which have been juxtaposed by the Variscan collision. Further on, the proposed Late Visean age for the phyllites has to be critically re-examined in the light of recently obtained Latest Visean $^{39}Ar/^{40}Ar$ cooling ages (DOBMEIER, 1998) and the emplacement age of the synkinematic Pormenaz monzogranite (BUSSY et al., 1998).

We favour an Ordovician age for the Greenstone Unit by comparing all pre-Variscan magmatic suites in the Aigulles Rouges massif and reinterpreting their palaeotectonic significance. According to ε_{Nd} studies and bulk rock chemistry, the former pyroxenites, lherzolites and N-type MORB basalts of the Lac Cornu area derived from a depleted mantle source and may have infiltrated a thinned continental crust (PFEIFER and VON RAUMER, 1996). PAQUETTE et al. (1989) interpreted a discordant U/Pb zircon age of 453 +3/–2 Ma as magmatic crystallization age. Amphibolites from the Lac d'Emosson chemically resemble basalts of continental rift zones with strong extension (VON RAUMER et al.,1990). Although the two occurrences of mafic rocks exhibit similar geochemical signatures and have about the same supposed age, their pre-orogenic relationship is yet unclear. VON RAUMER et al. (1990) and PFEIFER and VON RAUMER (1996) interpreted them together as remnants of an Ordovician continental rift zone. But a Cambro-Ordovician age is most likely as well for Hybrid-type and S-type metagranitoids of the Val Bérard area which indicate the existence of an active continental margin (WIRSING, 1997). Therefore the formation of the mafic to ultramafic rocks may rather be related to the initial stage of an active continental margin where extension accompanied by extensive mafic magmatism is prevalent (cf. PITCHER, 1993). The Greenstone Unit may well represent a different segment of the very same active margin, as the coexistence of oceanic island-arcs and active continental margins along the same subduction zone is well known (e.g. recent Sumatra-Banda arc seg-

ment in Southeastern Asia [HUTCHINSON, 1982]). Later on, both segments may have been juxtaposed along a transcurrent strike-slip dominated shear zone. In this context it is noteworthy that an oblique hypercollision occurred at least during the Visean (DOBMEIER, 1996; 1998). However, lack of absolute ages limits the reliability of every evolutionary model proposed for the Aiguilles Rouges massif. By that, the importance of future absolute age determinations in the Aiguilles Rouges massif becomes obvious.

In the frame of our proposed paleaotectonic setting and formation age, a correlation of the Greenstone Unit with the Chamrousse-Séchillienne ophiolitic complex seems viable if the latter is interpreted as remnant of a back-arc basin.

Acknowledgements

This paper presents results from a doctoral thesis (CD), which has been funded by the Erika-Giehrl-Stiftung, Erlangen and the Swiss National Science Foundation (Project No. 21-39181.93). Many thanks to F. Bussy (Lausanne) for assisting the microprobe analyses, M. Cosca and J. Hunziker (Lausanne) who helped a lot with the $^{39}Ar/^{40}Ar$ analyses, J.-C. Lavanchy (Lausanne) who assisted the XRF analyses, R.-P. Ménot (St-Etienne) for critical remarks during field trips and for scrutinizing the first draft of this paper, and P. Thélin (Lausanne) for informations about chlorites. A constructive review by D. Thiéblemont (Orleans) improved the manuscript decisively.

References

BELLIÈRE, J. and STREEL, M. (1980): Roches d'âge viséen supérieur dans le massif des Aiguilles Rouges (Haute-Savoie). C. R. Acad. Sci. Paris, 290 D, 1341–1343.

BUJAN, F. (1989): Le Carbonifère de Servoz-les Houches (Massif des Aiguilles Rouges). 111 pp., Trav. Diplôme Univ. Lausanne [unpubl.].

BUSSY, F., DELITROZ D., FELLAY, R. and HERNANDEZ, J. (1998): The Pormenaz monzonite (Aiguilles Rouges, Western Alps): an additional evidence for a 330 Ma-old magnesio-potassic magmatic suite in the Variscan Alps. Schweiz. Mineral. Petrogr. Mitt. 78, 193–194 (Poster abstract).

BUSSY, F. and HERNANDEZ, J. (1997): Short-lived bimodal magmatism at 307 my in the Mont-Blanc/Aiguilles-Rouges [sic] area: a combination of decompression melting, basaltic underplating and crustal fracturing. Quad. Geodinamica Alpina e Quaternaria, 4, 22 (Abstract).

CARME, F. and PIN, C. (1987): Vue d'ensemble sur le magmatisme pre-orogénique et l'évolution métamorphique et tectonique varisque dans le sud de la chaîne de Belledonne (Massifs cristallins externes, Alpes françaises). C. R. Acad. Sci. Paris, 304 II, 1177–1180.

COLOMBI, A. (1989): Métamorphisme et géochimie des roches mafiques des Alpes ouest-centrales (géoprofil Viège–Domodossola–Locarno). Mém. Géol. (Lausanne), 4, 216 pp.

CORBIN, P. and OULIANOFF, N. (1927): Sur les bésimaudites du Prarion (Haute-Savoie). C.R. Acad. Sci. Paris, 184, 892–894.

CULLERS, R.L. and GRAF, J.L. (1984): Rare earth elements in igneous rocks of the continental crust: Intermediate and acid rocks. 275–316 In: HENDERSON, P. (ed.): Rare earth geochemistry. Elsevier, Amsterdam a.o., 510 pp.

DEER, W.A., HOWIE, R.A. and ZUSSMAN, J. (1963): Rock forming minerals. Vol. 2 Chain silicates. Longman, London, 379 pp.

DEER, W.A., HOWIE, R.A. and ZUSSMAN, J. (1986): Rock-forming minerals. Vol. 1B. Disilicates and ring silicates. Longman, London, 629 pp. 2nd ed.

DOBMEIER, C. (1996): Die variskische Entwicklung des südwestlichen Aiguilles-Rouges Massivs (Westalpen, Frankreich). Mém. Géol. (Lausanne), 29, 191 pp.

DOBMEIER, C. (1998): Variscan P-T-deformation paths from the southwestern Aiguilles Rouges Massif (External massif, western Alps) and their implication for its tectonic evolution. Geol. Rundsch., 87, 107–123.

FIELD, D. and ELLIOTT, R.B. (1974): The chemistry of gabbro/amphibolite transitions in South Norway. Contrib. Mineral. Petrol., 47, 63–76.

FLOYD, P.A., WINCHESTER, J.A., CIESIELCZUK, J., LEWANDOWSKA, A., SZECZEPANSKI, J. and TURNIAK, K. (1996): Geochemistry of early Palaeozoic amphibolites from the Orlica-Śnieźnik dome, Bohemian massif: petrogenesis and paleotectonic aspects. Geol. Rundsch., 85, 225–238.

FRISCH, W., NEUBAUER, F., BRÖCKER, M., BRÜCKMANN, W. and HAISS, N. (1987): Interpretation of geochemical data from the Caledonian basement within the Austroalpine basement complex. In: FLÜGEL, H.W., SASSI, F.P. and GRECULA, P. (eds): Pre-Variscan and Variscan events in the Alpine-Mediterranean mountain belts. Alfa, Bratislava, 209–226.

GILL, J.B. (1981): Orogenic andesites and plate tectonics. Springer Verlag, Berlin a.o., 390 pp.

GAUCH, R.I. (1989): Rare earth elements in metamorphic rocks. – Rev. Mineral., 21, 147–167.

HAWKESWORTH, C.J., O'NIONS, R.K., PANKHURST, R.J., HAMILTON, P.J. and EVENSEN, N.M. (1977): A geochemical study of island arcs and back-arc tholeiites from the Scotia Sea. Earth Planet. Sci. Lett., 36, 253–262.

HOFMANN, A.W. (1988): Chemical differentiation of the Earth: the relationship between mantle, continental crust, and oceanic crust. Earth Planet. Sci. Lett., 90, 297–314.

HUTCHINSON, C.S. (1982): Indonesia. In: THORPE, R.S. (ed.): Andesites. Orogenic andesites and related rocks. Wiley & Sons, Chichester a.o., 207–224.

LAIRD, J. and ALBEE, A.L. (1981): Pressure, temperature and time indicators in mafic schist: their application to reconstruct the polymetamorphic history of Vermont. Amer. J. Sci., 281, 127–175.

LAURENT, R. (1967): Etude géologique et pétrographique de l'extrémité méridionale du massif des Aiguilles Rouges (Haute-Savoie, France). Arch. Sci. (Genève), 20, 227–354.

LEAKE, B.E. (1978): Nomenclature of amphiboles. Amer. Mineral., 63, 1023–1052.

LEAT, P.T., JACKSON, S.E., THORPE, R.S. and STILLMAN, C.J. (1986): Geochemistry of bimodal basalt-subalkaline/peralkaline rhyolite provinces within the Southern British Caledonides. J. Geol. Soc., London, 143, 259–273.

LIÉGEOIS, J.-P. and DUCHESNE, J.-C. (1981): The Lac Cornu retrograded eclogites (Aiguilles Rouges massif, Western Alps, France): evidence of crustal origin and metasomatic alteration. Lithos, 14, 35–48.

MÉNOT, R.P. (1987): Magmatismes paléozoïques et structuration carbonifère du massif de Belledonne (Alpes françaises). Contraintes nouvelles pour les schémas d'évolution de la chaîne varisque Ouest-Européenne. Mém. Doc. Centre Armor. Etudes Struct. Socles, Rennes, 1988, 465 pp.

MÉNOT, R.P. (1988): The geology of the Belledonne massif: an overview (External crystalline massifs of the Western Alps). Schweiz. Mineral. Petrogr. Mitt., 68, 531–542.

MÉNOT, R.P. and PAQUETTE, J.-L. (1993): Geodynamic significance of basic and bimodal magmatism in the External Domain. In: VON RAUMER, J.F. and NEUBAUER, F. (eds): Pre-Mesozoic geology in the Alps. Springer, Berlin a.o., 241–254.

MYASHIRO, A. (1974): Volcanic rock series in island arcs and active continental margins. Amer. J. Sci., 274, 321–355.

PAPIKE, J.J., CAMERON, K.L. and BALDWIN, K. (1974): Amphiboles and pyroxenes: Characterization of other than quadrilateral components and estimates of ferric iron from microprobe data. Geol. Soc. Amer. Abstr. with programs, 6, 1053–1054.

PAQUETTE, J.-L., MÉNOT, R.-P. and PEUCAT, J.-J. (1989): REE, Sm–Nd and U–Pb zircon study of eclogites from the Alpine External Massifs (Western Alps): evidence for crustal contamination. Earth Planet. Sci. Lett., 96, 181–198.

PEARCE, J.A. (1983): Role of the sub-continental lithosphere in magma genesis at active continental margins. In: HAWKESWORTH, C.J. and NORRY, M.J. (eds): Continental basalts and mantle xenoliths. Shiva, Nantwich, 230–249.

PEARCE, J.A. and NORRY, M.J. (1979): Petrogenetic implications of Ti, Zr, Y, and Nb variations in volcanic rocks. Contrib. Mineral. Petrol., 69, 33–47.

PFEIFER, H.-R. and VON RAUMER, J.F. (1996): Lherzolitic and pyroxenitic ultramafics from the Lac Cornu area (Aiguilles Rouges Massif, France). Schweiz. Mineral. Petrogr. Mitt., 76, 119 (Poster abstract).

PITCHER, W.S. (1993): The nature and origin of granite. Blackie Academic & Professional / Chapman & Hall, London a.o., 321 pp.

RAITH, M. (1976): The Al–Fe(III)Epidote miscibility gap in a metamorphic profile through the Penninic series of the Tauern Window, Austria. Contrib. Mineral. Petrol., 57, 99–117.

SCHULZ, B. and VON RAUMER, J.F. (1993): Syndeformational uplift of Variscan high pressure rocks (Col de Bérard, Aiguilles Rouges Massif, Western Alps). Z. dt. geol. Ges., 144, 104–120.

SUN, S.-S. and MCDONOUGH, W.F. (1989): Chemical and isotopic systematics of oceanic basalts: implications for mantle composition and processes. Geol. Soc. Spec. Publ., 42, 313–345.

THIÉBLEMONT, D., CHEVREMONT, P., CASTAING, C. and FEYBESSE, J.L. (1994): La discrimination géotectonique des roches magmatiques basiques par les éléments traces: reévaluation d'apres une base de données et application a la chaîne panafricaine du Togo. Geodinamica Acta, 7, 139–157.

THIÉBLEMONT, D. and TÉGYEY, M. (1994): Une discrimination géochimique des roches différenciées témoin de la diversité d'origine et de situation tectonique des magmas calco-alcalins. C.R. Acad. Sci. Paris, II, 319, 87–94.

THOMPSON, G. (1991): Metamorphic and hydrothermal processes: basalt-seawater interactions. In: FLOYD, P.A. (ed.): Oceanic basalts. Blackie, Glasgow a.o., 148–173.

TRIBOULET, C. (1992): The (Na–Ca) amphibole-albite-chlorite-epidote-quartz geothermometer in the system S–A–F–M–C–N–H_2O. 1. An empirical calibration. J. metamorphic Geol., 10, 545–556.

TRÖGER, W.E. (1967): Optische Bestimmung der gesteinsbildenden Minerale. Teil 2 Textband. Stuttgart (Schweizerbart) 822 S.

TSUCHIYA, N. (1990): Middle Miocene back-arc rift magmatism of basalt in the NE Japan arc. Bull. Geol. Surv. Japan, 41, 473–505.

VON RAUMER, J.F., GALETTI, G., PFEIFER, H.R. and OBERHÄNSLI, R. (1990): Amphibolites from Lake Emosson/Aiguilles Rouges, Switzerland: Tholeiitic basalts of a Paleozoic continental rift zone. Schweiz. Mineral. Petrogr. Mitt., 70, 419–435.

VON RAUMER, J.F., MÉNOT, R.P., ABRECHT, J. and BIINO, G. (1993): The pre-Alpine evolution of the External Massifs. In: VON RAUMER, J.F. and NEUBAUER, F. (eds): Pre-Mesozoic geology in the Alps. Springer, Berlin a.o., 221–240.

WILSON, M. (1989): Igneous petrogenesis – a global approach. Chapman & Hall, London a.o., 466 pp.

WINCHESTER, J.A. and FLOYD, P.A. (1977): Geochemical discrimination of different magma series and their differentiation products using immobile elements. Chem. Geol., 20, 325–343.

WIRSING, A. (1997): Die Orthogneise des oberen Val Bérard (Aiguilles-Rouges-Massiv, Westalpen, Frankreich). 142 pp, Doctoral Thesis Univ. Fribourg [unpubl.].

Manuscript received March 6, 1998; revision accepted April 8, 1999.